Supporting Online Material for

Quantitative 3D Video Microscopy of HIV Transfer Across T Cell Virological Synapses

Wolfgang Hübner, Gregory P. McNerney, Ping Chen, Benjamin M. Dale, Ronald E. Gordon, Frank Y. S. Chuang, Xiao-Dong Li, David M. Asmuth, Thomas Huser, Benjamin K. Chen*

*To whom correspondence should be addressed. E-mail: ben.chen@mssm.edu

Published 27 March 2009, *Science* **323**, 1743 (2009)
DOI: 10.1126/science.1168877

This PDF file includes:

Materials and Methods
Figs. S1 to S7
Tables S1 to S3
References

Other Supporting Online Material for this manuscript includes the following:
available at www.sciencemag.org/cgi/content/full/323/5922/1743/DC1

Movies S1 to S12

Supporting Online Material

Materials and methods

Viral constructs. HIV Gag-iGFP, Gag-iCerulean and Gag-iVenus are NL4-3-based (*1*) HIV-1 molecular clone that carrie respectively green fluorescent protein (GFP), Cerulean and Venus inserted internally into Gag between the MA and CA domains (*2*). HIV NL-GI is a molecular clone where EGFP replaces Nef in HIV NL4-3 and Nef is replaced downstream of an IRES (*3*). A variant expressing the Env gene from molecular clone JRFL (*4*) was constructed carrying the NdeI to BamHI fragment in NL4-3 replaced with the corresponding sequence from JRFL.

Cell to cell viral transfer assay. Viral transfer assays were carried out as described previously (*5*). Jurkat or primary T cells were transfected by electroporation with the HIV Gag-iGFP construct according to manufacturers instructions (Amaxa). Primary T cells were PHA activated for 3 days followed by 2 days growth in IL-2-containing medium prior the nucleofection. The donor cells were mixed with target CD4+ T cells at a 2:3 ratio. For flow cytometry analyses, the cells were incubated in a 5 ml round-bottom tube (BD Falcon).

Inhibitors of viral transfer and infectivity. Contact dependent infection was inhibited through separation of the two cell types with a 0.4 µm pore size Transwell (Corning Inc.). HIV Gag-iGFP-expressing Jurkat donor cells on top of the transwell and CellTracker blue CMF_2HC (Invitrogen)-labeled MT4 target cells at the bottom. For inhibitor assays, both donor and target cells were preincubated for 15 minutes at 37ºC prior coculture or incubation with cell-free virus. Cell-free virus was produced in 293T cells. 25ng p24 per 1 x 10^6 MT4 cells were used for cell-free infections. Actin inhibitor, cytochalasin D (BD Biosciences) was used at 2.5 µM final concentration. HIV-1 neutralizing serum 2 and negative control human serum (Catalog number 2411 and 1984 from Dr. Luba Vujcic through the AIDS Research and Reference Reagent Program (*6*)) were used at a 1:50 dilution. Both the serum and cytochalasin D treatment were carried out for a 19h period, after which all cells were washed and grown in media containing AMD3100. MT4 infection assays were stopped at 48h incubation after a 10 minutes trypsin treatment, followed by 4% paraformaldehyde fixation.

Immunofluorescence and laser scanning confocal imaging of fixed samples. Cells were mixed and left in culture on Poly-L-Lysine coated glass coverslips. They were fixed at the indicated times with 4% paraformaldehyde for 10 minutes and mounted with Vectashield hardset solution. Images of the fixed cells were acquired by laser scanning confocal microscopy on a Zeiss Axiovert 200 fitted with LSM510 META detectors or a Leica SP5M system. Immunofluorescence labeling was performed in surface staining or permeabilization conditions. For surface staining, the conjugated cells were mixed with a monoclonal anti-gp41 antibody, 50-69, at 1:100 dilution (from Dr. Susan Zolla-Pazner through the ARRP) for 30 minutes on ice. Cells were fixed and stained for secondary anti-human Texas Red conjugated antibody (Jackson ImmunoResearch Laboratories). For internal labeling, cells were immediately fixed in

4% paraformaldehyde for 10 minutes followed by permeabilization in 0.15% Triton-X100 for 3 minutes. The cells were blocked for 30min in a 3% BSA 0.2% fish gelatin 0.2% Tween 20 solution prior to the staining with human monoclonal 50-69 antibodies.

Electron microscopy. Cells were fixed with 3% glutaraldehyde in 0.2 M sodium cacodylate, pH 7.4. The specimens were then treated with 1% osmium tetroxide for 1 h, followed by ethanol dehydration in graded steps through propylene oxide, and then embedded in Embed 812 (Electron Microscopy Sciences, Hatfield, PA). Ultra-thin sections (70nm or 150nm thick) were stained with uranyl acetate and lead citrate. Images were acquired on a Hitachi H7000 transmission electron microscope.

FRET imaging. FRET was performed as described previously (14). Jurkat cells were cotransfected with HIV Gag-iCerulean (donor) and HIV Gag-iVenus (acceptor) constructs and used in viral transfer assays with CellTracker Orange (CMRA)-labeled CD4+ primary T cells and plated on Poly-L-Lysine coated coverslips. Spectral imaging was acquired with a Zeiss LSM510 META detector after fixation and mounting in Vectashield solution. The donor, FRET and acceptor images were generated after linear unmixing using the Zeiss LSM software v.3.2 according to the corresponding spectral profiles of HIV Gag-iCerulean and HIV Gag-iVenus. NFRET images were calculated using Volocity software (Improvision).

Live wide-field deconvolution imaging conditions. Jurkat donor and CD4+ target T cells were mixed, centrifuged at 300g for 5 minutes and plated into an uncoated gas-permeable ibidi chamber (μ-Slide VI; Ibidi Integrated BioDiagnostics) at a density that allowed the imaging of isolated donor-target cell pairs. In the uncoated chamber cells could form cell-cell conjugates without forming strong attachments to the bottom of the imaging chamber. 12 different 3D fields were imaged for 4 hours at 15 minute intervals using a personalDV deconvolution microscope (Applied Precision, Issaquah, WA) with a 40X 0.9 NA air objective and illumination by a Xenon arc lamp source. Green fluorescence (for GFP imaging) and phase contrast channels were used in sequence. System control and image collection was controlled by the SoftWoRx software (Applied Precision). A thermostatic heater (Nevtek) maintained a 37ºC environment throughout the experiment.

Spinning Disk confocal live imaging. After loading an ibidi imaging chamber with cells, it was immediately mounted on an Olympus iX71 inverted optical microscope. A thermostatic heater (Nevtek) maintained a 37ºC environment. Images were collected through a 60x 1.42 NA oil immersion objective and recorded by an iXon 897 EM-CCD camera (Andor Technologies, Ireland) attached to a CSU-10 spinning disk confocal unit (Yokagawa, Japan). Excitation wavelength selection, rapid on-off shuttering, and excitation power control of an Innova 70C Argon kryton ion gas laser (Coherent, Santa Clara) operating on all laser lines simultaneously was achieved by an Andor acousto-optic tunable filter. Data acquisition and hardware was controlled using Andor iQ v1.8. Live cell spinning disk fluorescence imaging was performed by selecting conjugated cell pairs over a period of up to 4-6h after mixing in the gas-permeable cell chamber. Selected infected cells were imaged for 20 to 60 minutes at a time. Full 3D stacks were

acquired at a rate of one per 1.2 to 1.9 seconds. Out of 43 observed HIV Gag-iGFP-expressing Jurkat cells, adhesions to CD4+ target cells occurred 29 times. 2 newly formed cell-cell adhesions and 4 new VS button formations were recorded. In 8 cases, movements of Gag puncta towards the synapse in the Jurkat donor cell were recorded. Transfer from the donor to the target was imaged in 10 conjugates (Table S2).

Laser scanning confocal live imaging. Jurkat donor cells expressing HIV Gag-iGFP were mixed with CMTMR-labeled acceptor CD4+ T cells and plated into an ibidi chamber. The chamber was placed on a Zeiss Axiovert 200 microscope with LSM 510 META detector and the temperature was maintained at 37°C using a thermostatic heater (Nevtek). Imaging of the conjugated Jurkat cell (Fig. 5) started one hour post mixing. A full 25µm stack was acquired every 5 minutes over 13 hours.

Long duration epifluorescence live imaging. Donor Jurkat cells expressing HIV Gag-iGFP and HIV NLGI were mixed with CMTMR-labeled acceptor cells into a Poly-L-Lysine coated ibidi chamber. The chamber was mounted in a heated enclosed CO_2 environment on an inverted Olympus IX-70 microscope (20x 0.45 NA air objective) fitted with a Evolution QEi monochrome CCD camera. InVivo Imaging software (MediaCyberbetics) was used for acquisition and control. 11 different fields were imaged every 10 minutes for green fluorescence and phase contrast for 67 hours. To minimize photobleaching, red channel CMTMR target cell label was acquired only at the beginning and at 25, 47 and 67 hours post mixing.

Image Analysis. Image analysis was performed with ImageJ (http://rsb.info.nih.gov/ij/) and Volocity (Improvision) on Macintosh computers (Apple, Inc). Spinning Disk Laser confocal images were intensity bleach corrected and deconvolved with Volocity. Intensity measurements and tracking of Gag puncta was performed with the Volocity Quantification module. The distance from the synapse and velocity of the tracked object were calculated by normalizing movements to the center of the synaptic button.

Supporting Figures

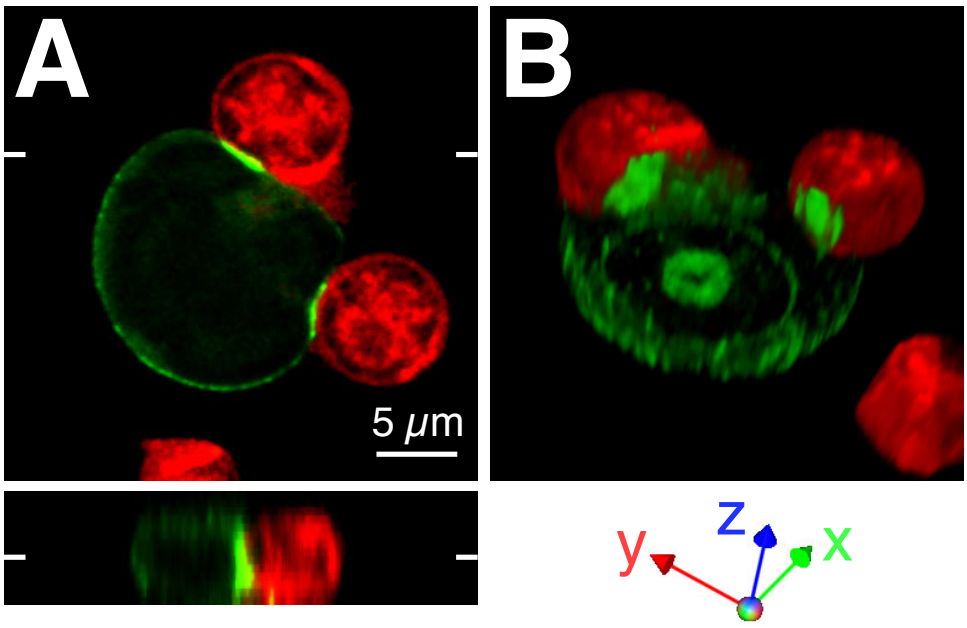

Fig. S1. Gag accumulates at synaptic buttons formed between primary CD4+ T cells. (**A**) Button formation observed between a HIV Gag-iGFP-expressing primary T cell and an autologous CD4+ T cell. Notches indicate the position of the XY (top) and XZ (bottom) perpendicular planes. (**B**) 3D reconstruction of synaptic buttons from A.

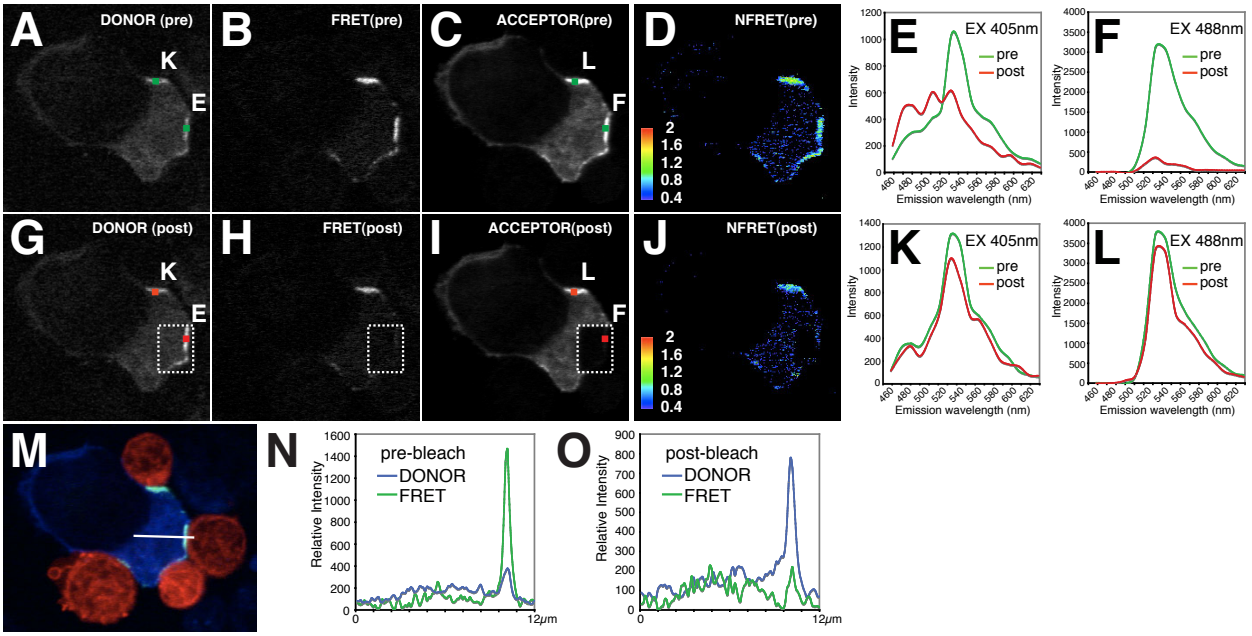

Fig. S2. Fluorescence resonance energy transfer analysis of HIV Gag-iCerulean (donor) and HIV Gag-iVenus (acceptor) fluorophores upon cotransfection into Jurkat T cells and cocultured with CD4+ T cells. (**A**) Donor emission when excited at 405 nm, (**B**) FRET emission resulting from an excitation at 405 nm, (**C**) acceptor emission when excited at 488nm, (**D**) normalized NFRET signal. (**E**) Spectral analysis of a region, **E**, at the cell-to-cell contact area pre- and post-photobleaching of the acceptor when excited at 405nm. (**F**) Spectral analysis of a region, **F**, at the cell to cell contact area pre and post photobleaching of the acceptor when excited at 488nm. (**G-J**) Images after irreversible photobleaching of the acceptor at 514nm in boxed area. (**K**) Lack of donor emission dequenching in region K, outside the region of acceptor bleaching when excited at 405nm. (**L**) The acceptor emission at 488nm excitation is not affected in region L outside the region of bleach. (**M**) Three-color overlay donor Cerulean fluorophore (blue, excitation at 405nm), FRET channel (green, excitation at 405nm) and CMTMR-stained target cells (red, excitation at 543nm). The intensity profile of the donor and FRET signals on line in M are plotted before (**M**) and after (**O**) acceptor photobleaching.

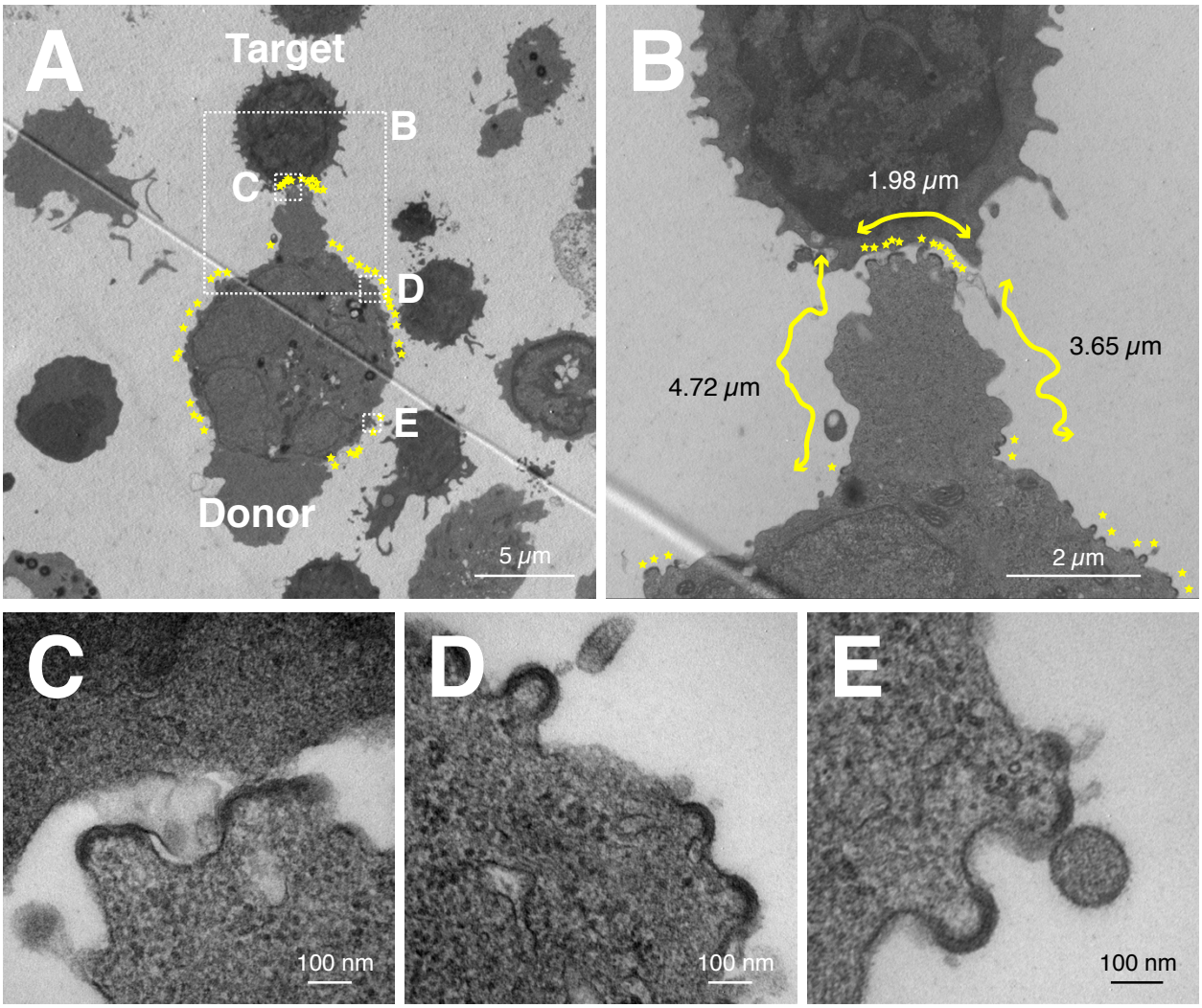

Fig. S3. Transmission electron microscopy of viral buds in 75nm sections tightly packed at the virological synapse and far from the cell-to-cell contact area. (**A**) HIV Gag-iGFP expressing Jurkat (Donor) is engaged in a virological synapse with a primary CD4+ T cell. Viral buds are marked by yellow stars at the cell surface. Locations of the high magnification views are indicated by the dotted line boxes. (**B**) Viral buds are very dense at the virological synapse. Other buds are observed far from the synapse at the indicated distances implying a zone of depletion around the Gag button-shaped accumulation. The diameter of the cell-to-cell contact zone is shown. (**C**) Higher magnification of viral buds at the virological synapse. (**D**-**E**) Higher magnification of viral buds at plasma membrane locations removed from the virological synapse.

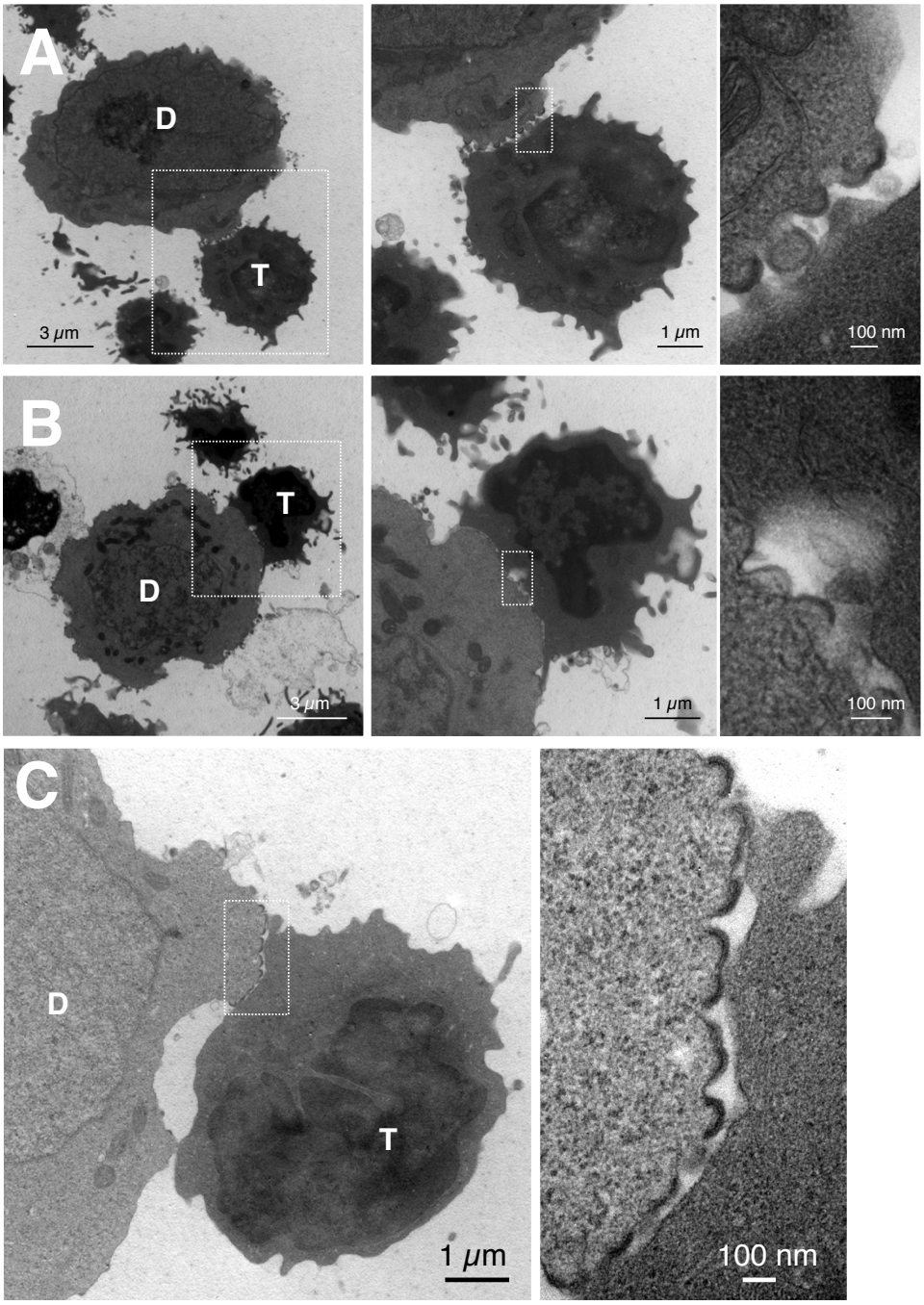

Fig. S4. Native HIV forms budding crescent forms at the virological synapse similar to those formed by HIV Gag-iGFP. (**A**) Donor cell crescents are nearly bud in this example. (**B**) An invagination in the target cell at this synapse. Donor Jurkat, D, and target CD4+ T cells, T, cells are indicated. Both images were acquired from 150 nm thick sections. Each panel represents a low magnification view (left) and successively higher magnifications from the white-dotted box (middle, right). **(C)** Images from 70 nm thick sections , low magnification (left) and a high magnification (right).

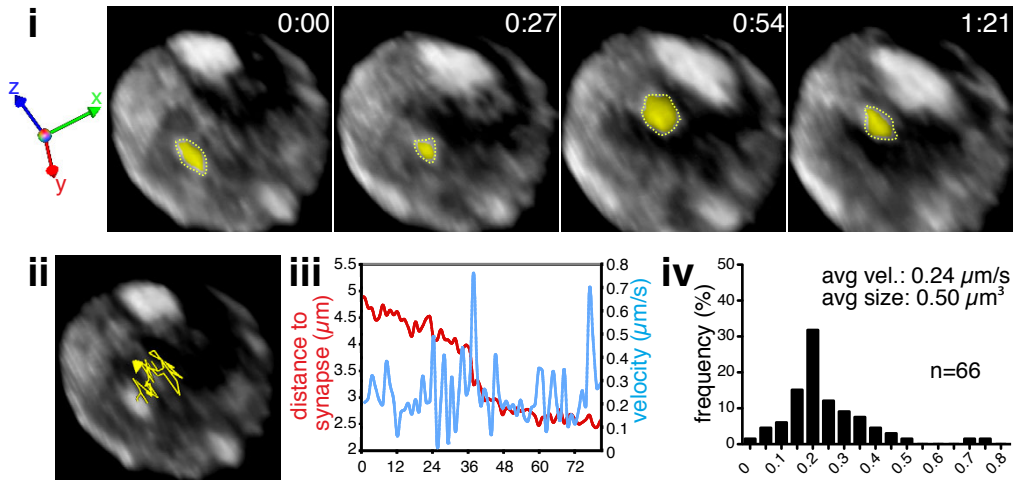

Fig. S5. Live 3D confocal fluorescence microscopy reveals rapid movement of Gag puncta towards the synapse. A small patch of membrane-associated Gag merges into the synapse from nearby sites. (i) Selected frames over 81 seconds illustrate movements of a highlighted (yellow) Gag-iGFP puncta. (ii) The path of the object overlayed on the original location of the object. (iii) The distance to the synapse, and the velocity of the object are graphed over time. (iv) The distribution of the velocities of the tracked objects is illustrated in a histogram plot.

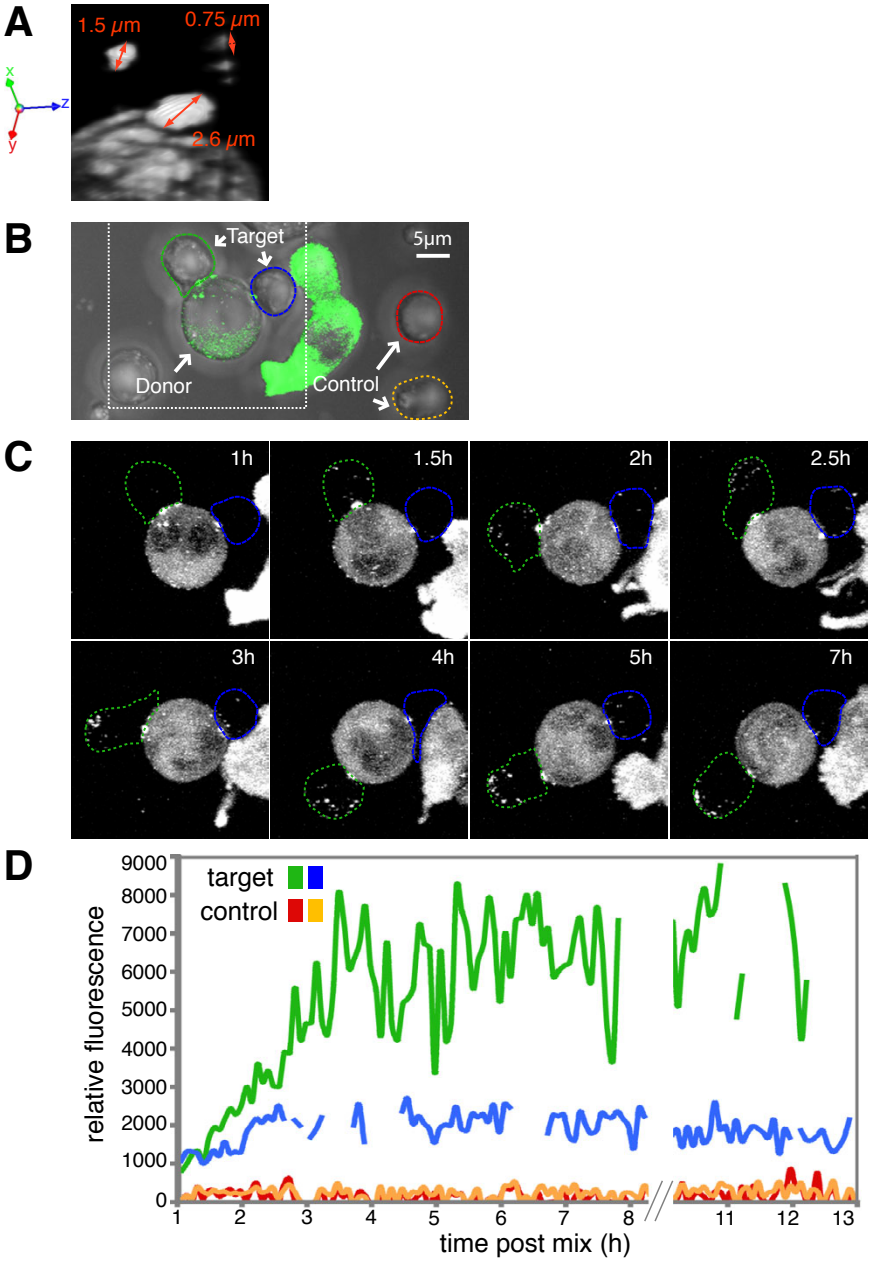

Fig. S6. The transferred Gag puncta can be large, accumulate over time in the CD4+ target T cell, and remain stable for over 13h. (**A**) Sizes of synaptic button and two transferred Gag puncta are illustrated in a 3D image. (**B**) Initial image of a 13h 3D laser scanning confocal sequence shows HIV Gag-iGFP-expressing Jurkat cell (donor) synapsed with two with target cells (dotted blue and green lines); HIV Gag-iGFP signal image (green) is overlayed on light transmission image in grayscale. (**C**) Images at indicated times following cell mixing document progressive accumulation of HIV Gag-iGFP in vesicular structures in the CD4+ target cells (dotted lines). (**D**) Integrated HIV Gag-iGFP signal accumulates in two target cells, but not in two control bystander cells and fluorescence is maintained over 13h.

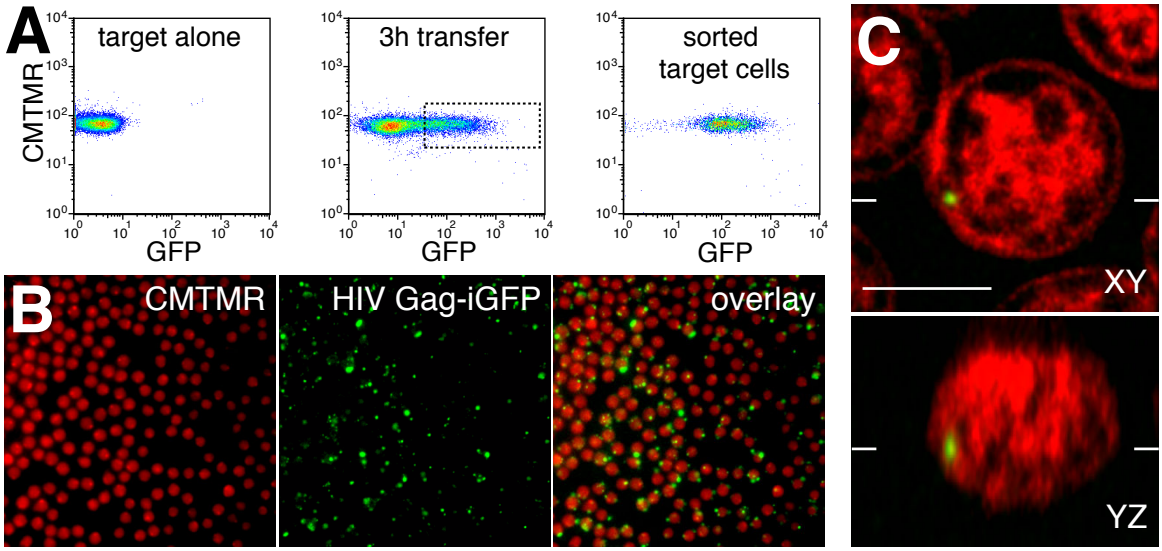

Fig. S7. Virological synapse-mediated accumulation of HIV Gag-iGFP targets an internal cellular compartment. **(A)** The HIV Gag-iGFP-positive CD4 target cells were sorted by flow cytometry after trypsin treatment. **(B)** Microscopy on the HIV Gag-iGFP-positive sorted cells exhibited punctate signals. **(C)** Confocal image of green HIV Gag-iGFP puncta within a CD4 target cell after synapse formation.

A **HIV Gag-iGFP**

fields[1]	HIV+ Jurkat cells in field at start[2]	HIV+ Jurkat cells in field at end[3]	target cells in conjugates[4]	button[5]	transfer[6]
1_01	9	8	1	1	0
1_02	12	11	3	3	1
1_03	10	9	0	0	0
1_04	11	9	1	1	0
1_05	9	9	3	3	0
1_06	6	8	1	1	1
1_07	8	5	2	0	0
1_08	10	8	4	3	0
1_09	6	6	1	1	1
1_10	9	9	3	2	1
1_11	9	11	2	2	0
1_12	11	7	3	3	1
totals	110	100	24	20	5

B **HIV Gag-iGFP ΔEnv**

fields[1]	HIV+ Jurkat cells in field at start[2]	HIV+ Jurkat cells in field at end[3]	target cells in conjugates[4]	button[5]	transfer[6]
2_01	8	8	0	0	0
2_02	13	14	0	0	0
2_03	12	11	0	0	0
2_04	16	15	0	0	0
2_05	13	13	0	0	0
2_06	11	8	0	0	0
2_07	11	11	0	0	0
2_08	10	10	0	0	0
2_09	12	11	0	0	0
2_10	13	12	0	0	0
2_11	16	17	0	0	0
2_12	7	7	0	0	0
totals	142	137	0	0	0

[1]Location on the cell chamber

[2]Number of GFP-positive cells at time 0

[3]Number of GFP-positive cells at 4h time point

[4]Number of target CD4+T cells conjugated for more than one time point to a GFP-positive Jurkat cell

[5]Number of donor cells with Gag accumulating in a button

[6]Number of target CD4+ T cells with GFP+ puncta

Table S1. Comparison of cell cell interactions by (**A**) HIVGag-iGFP-expressing versus (**B**) HIV Gag-iGFP ΔEnv-expressing cells. Four hour survey of cells in 12 fields of view, under live imaging conditions. Adhesion, button formation, and appearance of puncta in target cells is documented.

recording	adhesion[1]	new adhesion[2]	button at start[3]	new button[4]	donor puncta[5]	target puncta[6]	transfer[7]	start time (min post mix)[8]	duration (min)[9]
1_01								42	6
1_02	x		x			x	x	68	15
1_03	x(2)		x(2)			x	x	120	15
1_04	x		x					197	31
2_01	x		x					107	7
2_02	x		x			x	x	227	33
2_03								323	98
3_01	x		x					11	2
3_02								44	20
3_03	x		x					56	46
3_04	x		x		x	x	x	110	55
4_01								20	3
4_02								34	0
4_03								38	18
4_04	x		x					60	47
4_05	x			x				165	35
4_06	x			x				321	66
4_07	x		x			x	x	400	41
5_01								13	22
5_02	x		x					58	27
5_03	x		x		x			90	13
5_04	x		x					145	13
5_05	x		x					198	6
6_01	x	x		x	x	x	x	8	65
7_01								13	13
7_02								37	12
8_01								21	3
8_02	x		x		x			29	29
8_03	x		x		x			75	46
9_01	x		x					21	18
9_02								52	22
10_01								14	10
10_02	x		x			x	x	56	37
11_01								19	8
11_02	x		x			x	x	34	75
11_03	x(2)		x(2)			x		118	25
11_04	x		x					150	24
11_05								181	2
11_06	x		x		x	x	x	189	43
11_07								227	14
11_08	x	x		x	x			248	69
11_09								327	14
11_10	x		x		x	x	x	355	42
totals	**29**	**2**	**25**	**4**	**8**	**11**	**10**		**1187**

[1]A target cell and a donor cell are in a conjugate
[2]A new adhesion of a target cell to a Jurkat cell is recorded
[3]A pre-existing button is observed at the beginning of the recording
[4]The formation of a new Gag button is recorded
[5]Movement of Gag puncta towards the synapse are observed in the donor cell.
[6]Gag puncta are observed in the target cell from first image frame
[7]Transfer of Gag puncta from the donor to target cell is recorded
[8]Time of the start of the recording, elapsed time from initial cell mixing
[9]Duration of the recording (min)
[10]Events observed in each image series are marked with an x; x(2) indicates donor cells engaged with two targets

Table S2. Summary of rapid spinning disk confocal imaging acquired and enumeration of virological synapse events[10].

		t=1h10min					t=67h30min				
cell-associated	**field**	**HIV- Jurkat**	**HIV+ Jurkat**	**MT4 Target**	**conjugates**	**HIV+MT4**	**HIV- Jurkat**	**HIV+ Jurkat**	**MT4 Target**	**conjugates**	**HIV+ MT4**
NLGI/iGFP	1	34	11	116	4	0	89	9	134	3	0
	2	53	12	132	6	0	83	7	202	5	0
	3	47	15	110	11	0	71	5	155	0	1
	4	45	11	106	7	0	87	6	144	3	0
	5	35	13	111	11	0	75	9	146	9	1
	6	46	22	162	18	0	71	9	220	5	1
	7	46	28	125	14	0	72	12	181	3	0
	8	45	21	131	12	0	88	7	188	4	1
	9	54	20	164	15	0	98	5	224	3	0
	10	54	14	99	6	0	107	8	148	1	2
	11	50	18	103	8	0	109	12	160	5	1
totals		509	185	1359	112	0	950	89	1902	41	7

Table S3. Cell counts and interactions enumerated in 11 fields of view at 1h and 67h from a cell-associated HIV infection. HIVGag-iGFP-expressing Jurkat donor cells were mixed with MT4 target cells. Continuous imaging over 67 hours acquired at 10 minutes intervals allows retrospective tracking of the interactions of productively infected cells.

Supporting references

1. A. Adachi *et al.*, *J Virol* **59**, 284 (1986).
2. W. Hubner *et al.*, *J Virol* **81**, 12596 (2007).
3. G. B. Cohen *et al.*, *Immunity* **10**, 661 (1999).
4. W. A. O'Brien *et al.*, *Nature* **348**, 69 (1990).
5. P. Chen, W. Hubner, M. A. Spinelli, B. K. Chen, *J Virol* **81**, 12582 (2007).
6. L. K. Vujcic, G. V. Quinnan, Jr., *AIDS Res Hum Retroviruses* **11**, 783 (1995).

Online supporting materials

Materials and Methods, Figs. S1, S2, S3, S4, S5, S6, S7 and Tables S1, S2, S3

Supporting Movies

Movie S1.
Synaptic buttons are intense accumulations of Gag at the virological synapse, visualized here in a three-dimensional representation of an HIV Gag-iGFP-expressing Jurkat cell attached to three CD4+ target cells (red). HIV Gag-iGFP (green) is focused at the sites of cell-cell contact.

Movie S2.
Oligomerization of Gag at the virological synapse is detected by fluorescence resonance energy transfer between HIV Gag-iCerulean and HIV Gag-iVenus. Three-dimensional reconstruction with donor cerulean signal (blue) and FRET signal (green) shown in the HIV-expressing cell. CD4+ target cells are visualized with the fluorescent dye CMRA (red).

Movie S3.
Formation of a synaptic button at a site where a target cell has recently attached to a donor cell. Brief animation illustrates the perspective of the 3D reconstruction, followed by the movie in 3D view. The new button forms by movement of nearby Gag-iGFP towards the site of cell-cell contact. Spinning disc confocal images were recorded at one stack per 1.4 sec. Elapsed time is depicted in minutes:seconds.

Movie S4.
Overview spinning disc confocal movie of a synapse that displays the recruitment of Gag to a synaptic button, followed by the coordinated budding and endocytosis into the CD4+ target cell. Maximum intensity projection shown first, followed by a 3D reconstruction of the same images. Elapsed time is depicted in minutes:seconds.

Movie S5.
Movement of a vesicular Gag puncta into the virological synapse. Same puncta shown first without, then with, the object highlighted in a 3D reconstruction. Elapsed time is depicted in minutes:seconds.

Movie S6.
Coalescing of Gag puncta, and vectorial movement into the virological synapse. Same puncta is first shown first without, then with, the object highlighted in a 3D reconstruction. Elapsed time is depicted in minutes:seconds.

Movie S7.
Rapid movement of a small puncta out of and back into the synaptic button. 3D reconstruction image is first shown without, then with, the object highlighted. Elapsed time is depicted in minutes:seconds.

Movie S8.
Budding of large HIV Gag-iGFP-containing vesicles into CD4+ target cells is followed by vectorial movement of the HIV-laden compartment toward the distal pole of the cell. 3D reconstruction image shown first without, then with, the object highlighted. Elapsed time is depicted in minutes:seconds.

Movie S9.
Transfer of an entire synaptic button to the CD4+ target cell. Image is an overlay of brightfield image and green fluorescence in a maximum intensity projection of the acquired stack. Elapsed time is depicted in minutes:seconds.

Movie S10.
Accumulation of HIV Gag-iGFP (green) virus particles in target cells recorded with laser scanning confocal microscopy. 3D stack acquired every 5 minutes for 13 hours. Elapsed time is depicted in hours:minutes:seconds.

Movie S11.
Productive infection of VS target cells is observed with long duration wide field microscopy, cell #1 from Fig. 4A. Images acquired every 10 minutes over 67 hours. The HIV green fluorescence signal alone is on the left while an overlay of green fluorescence and phase contrast is shown on the right. Elapsed time is depicted in hours:minutes.

Movie S12.
After contact with HIV-infected cells, productive infection is observed in long duration imaging of cells #2 through #5 depicted in Fig. 4B. Images acquired with long duration wide field microscopy every 10 minutes over 67 hours. Elapsed time for each individual cells is depicted in hours:minutes.